water

MDPI

Article

Feasibility of Achieving Efficient Nitrite Accumulation in Moving Bed Biofilm Reactor: The Influencing Factors, Microbial Structures, and Biofilm Characteristics

Hongyi Li [1,*], Zhaoxia Xue [2,3,*], Tongxin Yin [2,3], Tingfeng Liu [1] and Zhixin Hu [1]

[1] School of Environmental Engineering, Nanjing Institute of Technology, Nanjing 211167, China
[2] Key Laboratory of Integrated Regulation and Resource Development on Shallow Lakes, Ministry of Education, Hohai University, Nanjing 210098, China
[3] College of Environment, Hohai University, Nanjing 210098, China
* Correspondence: hjlihongyi@njit.edu.cn (H.L.); xuezhx@hhu.edu.cn (Z.X.)

Abstract: Moving bed biofilm reactor (MBBR) is considered as a promising technology for wastewater treatment owing to the high biomass retention and low cost. In this study, the performance of using MBBR for partial denitrification (PD) was investigated. Denitrifying biofilm was successfully formed after 40 days with the biomass and nitrite reduction rate of 40.83 mg VSS/g carriers and 51.52 mg N/(gVSS·h), respectively. Morphology analysis by scanning electron microscope (SEM) showed that the biofilm surface was dominant by *cocci*, filamentous bacteria, and extracellular polymeric substances (EPS). Investigation about the influencing factors of PD found that the optimal COD/NO_3^--N and pH for efficient nitrite production (nitrate to nitrite ratio: 96.49%) was 3 and 9, respectively. Moreover, *Saccharimonadales* was proved to be dominant functional microbes in the constructed PD systems with different influent conditions because its relative abundance exhibited good correlation with the nitrite accumulation. By analyzing the biofilm characteristics under different conditions, PD was observed to mainly occur in the range of 300–700 µm inside the biofilm, where most of the dissolved oxygen was consumed. This study confirmed the feasibility and superior performance of PD-MBBR system.

Keywords: moving bed biofilm reactor; partial denitrification; nitrite accumulation; glycerol; *Saccharibacteria* species

Citation: Li, H.; Xue, Z.; Yin, T.; Liu, T.; Hu, Z. Feasibility of Achieving Efficient Nitrite Accumulation in Moving Bed Biofilm Reactor: The Influencing Factors, Microbial Structures, and Biofilm Characteristics. *Water* **2023**, *15*, 998. https://doi.org/10.3390/w15050998

Academic Editor: Jesus Gonzalez-Lopez

Received: 13 February 2023
Revised: 2 March 2023
Accepted: 2 March 2023
Published: 6 March 2023

1. Introduction

Anaerobic ammonium oxidation (anammox) has been proved as an efficient and cost saving biological nitrogen removal process, in which NO_2^--N is needed as one of the necessary substrates [1]. Therefore, the anammox process need to be combined with NO_2^--N process. Partial nitrification (ammonia to nitrite) has been widely used for NO_2^--N production in treating ammonia-rich wastewater [2]. But when treating low ammonia wastewater (e.g., municipal wastewater), the NO_2^--N accumulation was difficult to achieve because of the failure of suppressing nitrite oxidizing bacteria. For example, the inhibition of free ammonia (FA) and free nitrous acid (FNA) on nitrite oxidizing bacteria was more serious compared to ammonia oxidizing bacteria, therefore, FA and FNA were considered as effective control parameters to achieve partial nitrification. However, the low ammonia concentration in municipal wastewater cannot produce enough free ammonia (FA) and free nitrous acid (FNA) for this suppression. On the other side, the relative abundance of organics in the municipal wastewater provides an ideal condition for the growth of heterotrophic denitrifying bacteria, which would compete nitrite with anammox bacteria and compete oxygen with ammonia oxidizing bacteria [3].

The NO_2^--N accumulation is commonly observed in the denitrification process, and NO_2^--N accumulation is affected by many factors [4,5]. Recently, some studies aimed to

achieve efficient nitrite production via partial denitrification (PD) by metabolic control, i.e., nitrate was reduced to nitrite without further reduction in denitrification process. For example, some studies reported that the type of carbon source and COD/NO_3^--N (C/N) was closely related to the NO_2^--N accumulation in PD process. In acetate-driven PD system, the nitrate-to-nitrite transformation ratio (NTR) was reported up to 80% by C/N control [6–8]. Additionally, glucose and ethanol were also reported to be effective for PD process [9,10]. Moreover, the effect of pH was also important [11], and most acetate-driven PD process required pH control for efficient NO_2^--N production. Recently, glycerol as the carbon source of partial denitrification has been reported to achieve ~90% NTR without pH and C/N control [12], which was worthy for more deep investigation. Moreover, the microbial community of denitrifying bacteria also has important influence on PD process. *Thauera* and *Halomonas* were reported to be the dominant genera in acetate-driven PD system [6,13], while *Candidatus saccharibacteria* was found to be enriched in glucose-driven PD system [14]. In general, compared with the partial nitrification process, PD technology was considered easier to achieve in the engineering application without the complicated control strategies. However, the present studies about PD technology mainly focused on the higher and stable nitrite accumulation, but little of them comprehensively investigated the reactor configuration of PD system.

At present, the biological wastewater treatment technology is dominated by activated sludge process, such as A^2/O, sequencing batch reactor (SBR) and oxidation ditch, which faces problems such as high energy costs and vulnerability to impact loads [15]. Moving bed biofilm reactor (MBBR) gradually attracts more attention because of its significant advantages over traditional suspended activated sludge system, such as the higher biomass retention and lower cost [16]. Moreover, using MBBR technology for NO_2^--N production in PD reaction has special advantages. For example, the attached microorganisms in biofilm have higher carbon source utilization rate according to the previous studies [17]. In addition, Liu et al. (2023) [18] found that both the soluble extracellular polymeric substances (EPS) and bound EPS in biofilm were significantly higher than that in activated sludge. The degradable EPS produced in MBBR system could be used as carbon source when the influent carbon source was insufficient [19], thereby improving the denitrification efficiency. Moreover, the organic matter and dissolved oxygen (DO) usually cause heterotrophic denitrifying bacteria to compete with anammox bacteria for growth space and further inhibit the anammox activity [20]. The substrate gradient caused by the mass transfer limitations in MBBR could provide an ideal growth environment with low DO and chemical oxygen demand (COD) concentration for anammox bacteria when coupling with anammox process for nitrogen removal. Therefore, coupling PD with MBBR might be a promising technology for stable NO_2^--N production in engineering application.

In this study, glycerol-driven PD process was constructed based on MBBR system. First, denitrifying biofilm was formed in a MBBR using glycerol as the carbon source. In this stage, the growth of biofilm on biocarriers and the pollutants removal performance was investigated, also, the morphology of the mature PD biofilm was observed by scanning electron microscope (SEM). Then, the influence of C/N and pH value on PD-MBBR system were comprehensively investigated by evaluating the NO_2^--N accumulation performance, probing the microbial community structure, and analyzing the pollutant removal rules in the biofilm. This study will provide a theoretical basis for the stable and efficient accumulation of NO_2^--N in denitrification MBBR, which will also support the development of PD-Anammox technology in MBBR.

2. Materials and Methods

2.1. Construction and Operation of Denitrification MBBR

To investigate the influencing factors of PD-MBBR system, the denitrifying biofilm on biocarriers was first cultivated. Denitrification MBBRs used in this study were made of organic glass with the diameter and height of 20 cm and 30 cm, respectively. The working volume of MBBR was about 8 L with the drainage ratio of 0.625, and the temperature in the

reactor was kept at 35 ± 2 °C by water bath. The reactor was operated in sequencing batch mode with the operation cycle of 6 h, including 15 min for influent, 4 h for stirring, 30 min for settling, 30 min for drainage, and 45 min for idle.

The inoculated sludge of MBBR was taken from a glycerol-driven denitrification reactor which was operated for more than one year with the influent C/N of 5 and NO_3^--N removal rate of 18.94 mg/(gVSS·h). The MBBR was fed with synthetic wastewater, which was composed of glycerol (246.5 mg/L), $NaNO_3$ (364.3 mg/L), KH_2PO_4 (11.1 mg/L), $MgSO_4$ (6.0 mg/L), $CaCl_2$ (3.0 mg/L), and 1 mL/L trace elements solution [12]. Moreover, the synthetic wastewater was flushed with nitrogen gas before introducing to the reactor to reduce the oxygen. The size, density, bulk density, and specific surface area of the carriers (Wuxi Baiyuan Environmental Equipment Co., Ltd., Wuxi, China) were 25 mm, 0.96 g/cm^3 and 125 kg/m^3, respectively. The filling rate of MBBR was about 40%.

2.2. Influence of C/N and pH on the NO_2^--N Accumulation in MBBR

After stable operation for another 20 days when the biofilm was successfully formed, the effect of key influencing parameters on the denitrification NO_2^--N accumulation was studied. First, the effect of influent C/N on NO_2^--N accumulation was investigated. Five MBBRs with the C/N of 2, 3, 4, 5, and 6 were conducted. The pH value and NO_3^--N concentration was 7 and 60 mg/L, respectively. After the MBBR was operated for 20 days, the nitrogen transformation characteristics in one typical cycle were studied. Specifically, the reactors were sampled at 0, 5, 10, 15, 20, 30, 45, 60, 75, 90, 120, 150, 180, 210, and 240 min respectively to determine the NO_3^--N reduction and NO_2^--N accumulation during denitrification, also, COD concentration was measured to investigate the utilizing patterns of glycerol. Another four MBBRs were used to reveal the effect of influent pH on the NO_2^--N accumulation. The influent C/N was set as 3, which was the best obtained C/N for NO_2^--N in the previous experiment. The influent NO_3^--N concentration was 60 mg/L, and the influent pH was controlled at 6, 7, 8, and 9 by 5 mM HCl and NaOH. After the MBBRs were operated for 20 days, NO_3^--N, NO_2^-N, and COD were measured as described before.

2.3. Analytical Methods

NO_3^--N, NO_2^--N, NH_4^+-N, VSS, and COD in the samples were measured according to the standard method [21] after being filtered by Millipore filter units (pore size, 0.45 μm). The DO and pH were measured using portable DO and pH meters. The amount of biofilm was determined by the weighing method. Briefly, biocarriers from the reactor were treated with 1 mM NaOH solution ultrasonic treatment for 5 min to destroy the adhesive structure of the biofilm. Then, the volume of the obtained suspended biofilm was determined according to the measurement method of VSS. The biofilm thickness on the carrier surface and migration of material within the biofilm was determined by microelectrode detection.

The differences in microbial community structure between MBBRs with different influent parameters were disclosed by Illumina MiSeq technique. Specifically, the biofilm samples in carriers were collected on day 0, 20, 50, and 90 from the MBBRs. Total genomic DNA was extracted using the CTAB/SDS method. 341F-806R primer set was used to amplify 16S rRNA genes of the 16S V3-V4 regions. PCR products was mixed in equidensity ratios. Then, mixture PCR products was purified with GeneJET Gel Extraction Kit (Thermo Scientific, Waltham, MA, USA). Sequencing libraries were generated using NEB Next®Ultra™DNA Library Prep Kit for Illumina (New England Biolabs, Ipswich, MA, USA) following manufacturer's recommendations and index codes were added. For other procedures refer to Zhang et al. (2023) [22]. Sequences analyses were performed by UPARSE software package using the UPARSE-OTU and UPARSE-OTUref algorithms. Sequences with ≥97% similarity were assigned to the same OTUs. The community structure composition at each taxonomic level was determined by SILVA database (http://www.arbsilva.de) (accessed on 28 June 2021). Moreover, Chao, Shannon, and Simpson indices were calculated to evaluate the microbial diversity and richness of the sample.

2.4. Statistical Analysis

All the measurements were performed in triplicate, and statistical analysis including linear regression was conducted by IBM SPSS software. Graphs in this study was plotted by Origin software. And p value < 0.05 was considered significant when the obtained results were compared.

3. Results and Discussions

3.1. Start-Up of PD-MBBR

3.1.1. Variation of the Attached Biomass

The variation in the attached biomass on the surface of carriers during the start-up stage is shown in Figure 1a. In the first 20 days, the biomass increased slowly because the carrier surface was relatively smooth, which was disadvantageous to the attachment of the biofilm. However, EPS produced by microorganisms could gradually improve the surface performance of the carriers [23], which provided favorable conditions for the subsequent attachment and growth of microorganisms. Therefore, after the suspended sludge was emptied in 20 days, the attached biomass increased rapidly from 5.81 mgVSS/g carriers to 37.26 mgVSS/g carriers in 20~35 d, indicating that the formation of biofilm mainly resulted from the growth and reproduction of the attached microorganisms rather than the adhesion of the suspended microorganisms. The removal of suspended microorganisms enhanced the nutrient utilization of attached microorganisms, and finally, the biomass reached 40.83 mgVSS/g carriers at 40 d.

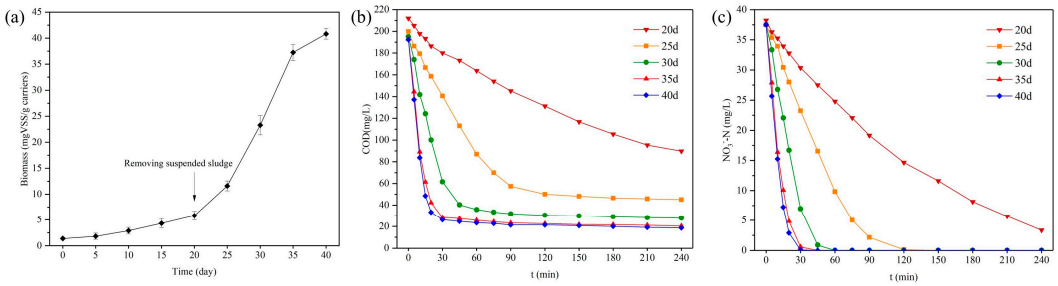

Figure 1. Variation of attached biomass on carriers (**a**) and removal of COD and NO_3-N in different periods (**b**,**c**).

3.1.2. Pollutants Removal Performance

After the suspended sludge was removed at 20 d, the pollutant removal ability of the reactor was tested. The changes in COD and NO_3^--N concentrations in one cycle are shown in Figure 1b,c. With the formation of biofilm, the removal rates of COD and NO_3^--N were improved. The NO_3^--N reduction rate increased significantly from 30.51 mg N/(gVSS·h) to 53.58 mg N/(gVSS·h) during 20 to 35 d. At 40 d, the NO_3^--N reduction rate was stabilized at 51.52 mg N/(gVSS·h), and NO_3^--N can be completely removed after one cycle of operation of the reactor. Meanwhile, the attached biomass was gradually stable, which indicated that the denitrifying biofilm formation was basically completed.

3.1.3. Biofilm Surface Features

At 40 d, the morphology of biofilm is shown in Figure 2. It can be seen that the biofilm inside the carriers was relatively dense, and the biofilm was yellow. Furthermore, the biofilm on the carriers was characterized by SEM. It could be seen that the biofilm was dominated by tightly bound cocci. Filamentous bacteria, as the bridge between cocci, were also observed. And the EPS secreted by microorganisms closely covered the surface of carriers.

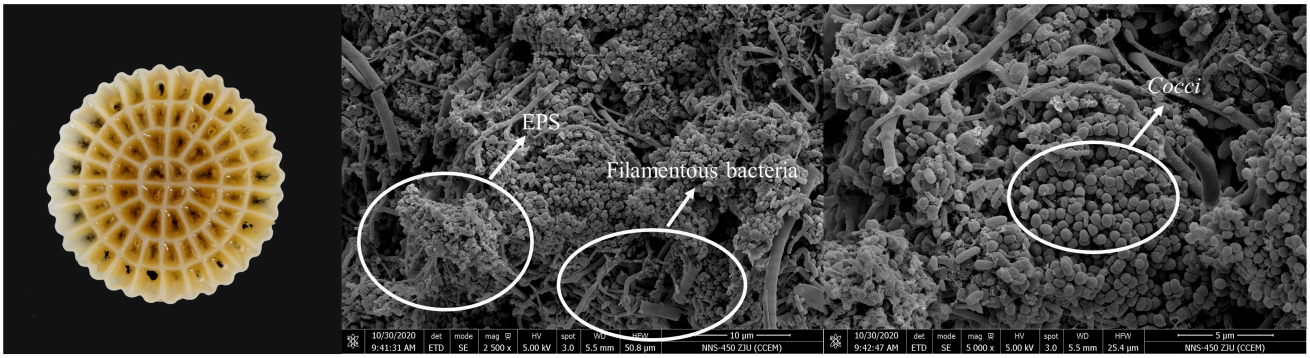

Figure 2. Morphology of the biofilm on biocarriers.

3.2. Effect of Influent C/N on PD-MBBR

3.2.1. NO_2^--N Accumulation Performance

At different influent C/N, the nitrogen transformation in denitrification MBBRs with glycerol as carbon source is shown in Figure 3. When the influent C/N was 2 and 3, owing to the carbon source was relatively sufficient at the initial stage of the reaction, the NO_3^--N was therefore rapidly reduced to NO_2^--N. The corresponding maximum NO_2^--N concentration reached 24.56 and 29.26 mg/L, respectively. Subsequently, the easily degradable carbon source was basically exhausted, and the remaining carbon source was difficult to be utilized by microorganisms. Therefore, the system entered the endogenous denitrification stage, of which the denitrification rate was extremely slow. At the end of 240 min, there was still NO_2^--N remaining in the system (20.18 mg/L at C/N of 2 and 24.20 mg/L at C/N of 3). When C/N $\geq$ 4, the influent carbon source was sufficient all the time, and NO_3^--N can be completely reduced in one cycle. The accumulation of NO_2^--N reached the maximum at 30, 30, and 20 min with the C/N of 4, 5, and 6, respectively. When the influent C/N was 6, the maximum accumulation of NO_2^--N reached 31.60 mg/L at 20 min, which was less than that when C/N was 5 (32.61 mg/L at 30 min). This was because the carbon source was more sufficient and the denitrification rate was higher when the influent C/N was 6, allowing more NO_2^--N to be reduced in the first stage. Consequently, C/N of 3 was considered as the optimal C/N in this study. On the other side, NTR, the key parameter of partial denitrification, only decreased from 90.41% to 85.88%, indicating the wide applicable range of C/N in engineering application. Moreover, it could be seen that NO_2^--N continued to decrease after the COD was almost exhausted. This might be because the biofilm contained a large number of biodegradable EPS, which could be used as a carbon source by denitrifying bacteria when the carbon source was insufficient [23]. The present results indicated that the precise control of influent C/N was extremely important to avoid the NO_2^--N loss in the engineering application.

As shown in Figure 3, glycerol, as a readily degradable carbon source, was quickly used at the initial stage of the reaction, therefore the COD concentration decreased rapidly. For example, the complete reduction of NO_3^--N to NO_2^--N making the COD concentration decreased from 187.5 mg/L to 21.2 mg/L at the C/N of 5. Theoretically, the conversion of 1 mg NO_3^--N to NO_2^--N required 1.15 mg COD [24], that is, the required COD was only 43.1 mg/L for the complete conversion of NO_3^--N, which was much lower than the actual consumption of 166.3 mg/L, indicating that most of the carbon source was not used for denitrification, but was absorbed by microorganisms or stored in cells.

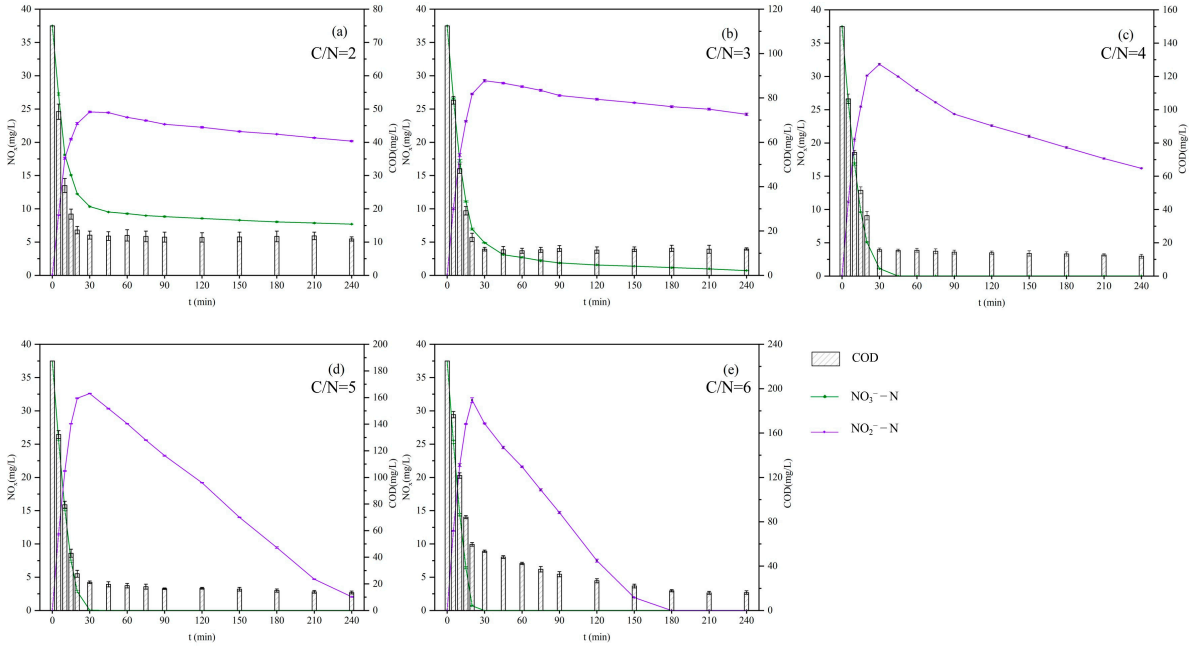

Figure 3. Changes of substrate concentration under different influent C/N: (**a**) 2; (**b**) 3; (**c**) 4; (**d**) 5; (**e**) 6.

3.2.2. Microbial Community

The difference of microbial community structure in denitrifying MBBR under different influent C/N was studied by high-throughput sequencing technology. Generally, 30,792–51,309 valid sequences were obtained, with an average length of 417–423 bp. OUT clustering was performed on the sequences according to 97% similarity, and the results were shown in Table 1. Chao index is used to estimate the total number of species, Shannon index and Simpson index are used to estimate the diversity of microorganisms. Chao and Shannon indices increased with the increase of influent C/N, while Simpson index was opposite, which indicated that the total number of species and microbial diversity increase continuously. This was because adequate influent carbon source was conducive to the growth of various microorganisms.

Table 1. Alpha diversity of biofilm under different influent C/N.

Sample	Reads	Index (Similarity: 97%)				
		OTU	Chao	Coverage	Shannon	Simpson
R1 (C/N = 2)	47,201	448	472	0.999	4.09	0.0491
R2 (C/N = 3)	51,309	464	484	0.999	4.38	0.0300
R3 (C/N = 4)	41,178	470	504	0.999	4.44	0.0248
R4 (C/N = 5)	30,792	475	514	0.998	4.49	0.0246
R5 (C/N = 6)	45,565	482	519	0.999	4.51	0.0241

The biofilm microbial community structure at the genus level is shown in Figure 4. The relative abundance of *Saccharimonadales* was 35.87%, 32.73%, 28.49%, 23.98%, and 21.25% at the influent C/N of 2, 3, 4, 5, and 6, respectively. *Saccharimonadale* has been reported to be denitrifying bacterium [25], which was capable of utilizing complex carbon sources and refractory organics [26]. Remmas et al. (2017) [27] found that *Saccharimonadales* was dominant in a membrane bioreactor with glycerol as carbon source, indicating that *Saccharimonadales* can utilize glycerol for growth. Moreover, some studies have found that *Saccharimonadales* was the dominant genus in the partial denitrification system with glucose as the carbon source [14]. Moreover, *Comamonadaceae*, *Denitratisoma*, and *Thauera* were also enriched in the system, which were reported to be the denitrifying bacteria

affiliated to the *Proteobacteria* phylum [10,28]. *Thauera* were the most common dominant bacteria in the partial denitrification system with sodium acetate and ethanol as carbon sources [10]. However, the relative abundance of *Thauera* was significantly lower than that of *Saccharimonadales* in this study, which indicated that the type of carbon source played a decisive role in the microbial structure of partial denitrification system.

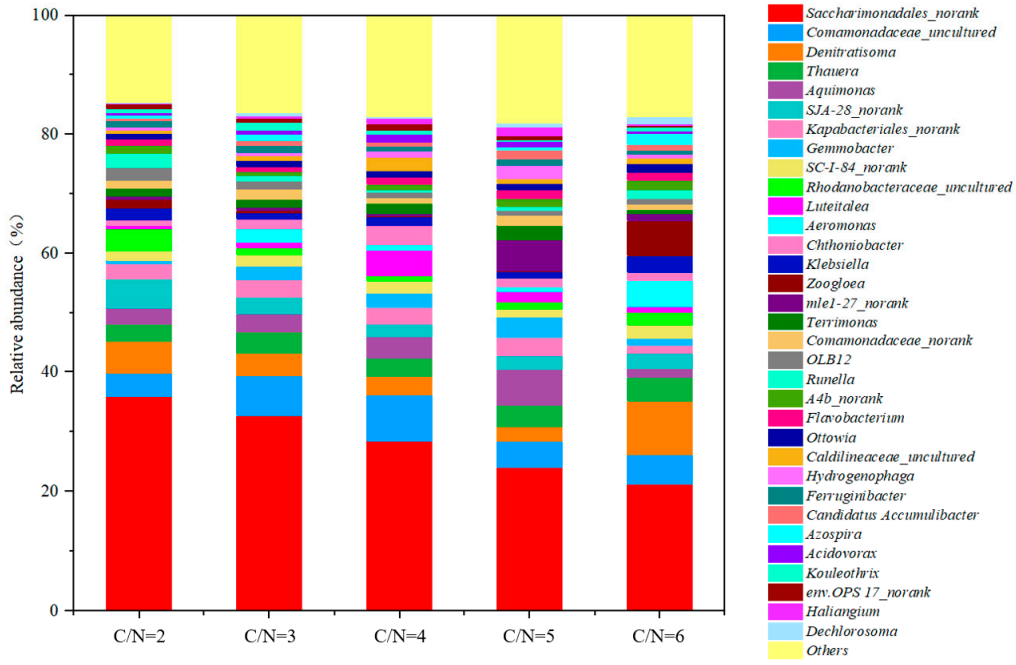

Figure 4. Microbial community structure of biofilm under different influent C/N (genus level).

3.2.3. Biofilm Characteristic

The biofilm thickness and the migration of substances inside the biofilm were analyzed by microelectrode (Figure 5). In the MBBRs with influent C/N of 2, 3, 4, 5, and 6, the mature biofilm thickness was 1200, 1200, 1300, 1400, and 1400 μm, respectively. The biofilm thickness increased with the influent C/N because sufficient carbon source promoted the growth of microorganisms.

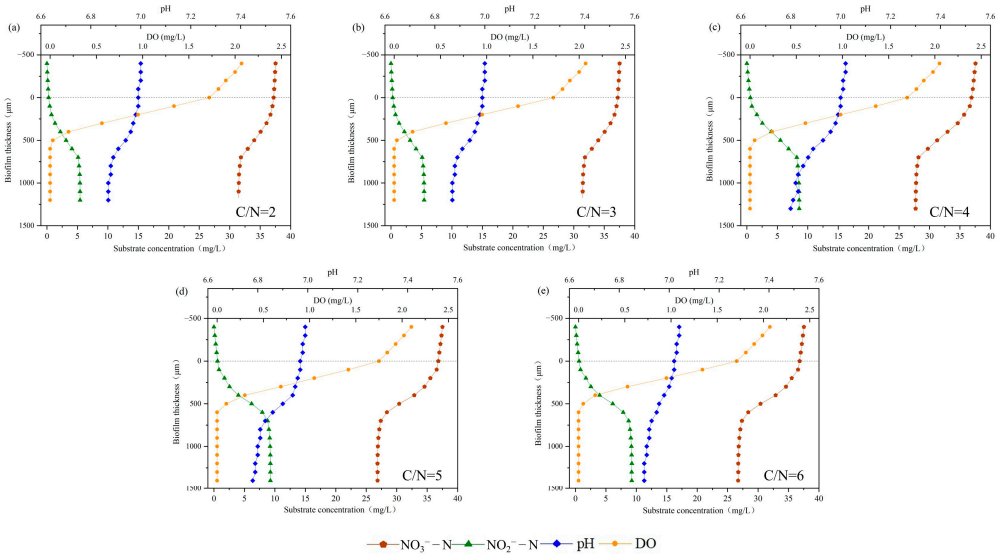

Figure 5. Biofilm thickness and the variation of substrate at different influent C/N: (**a**) 2; (**b**) 3; (**c**) 4; (**d**) 5; (**e**) 6.

In denitrification process, DO was used as an electron acceptor before NO_3^--N [29], so the DO decreased rapidly to 0.5 mg/L at 300~400 μm in the biofilm, which created the anoxic conditions for denitrification. The concentration of NO_3^--N decreased greatly in the range of 300~700 μm inside the biofilm, and NO_2^--N accumulated continuously, indicating that denitrification mainly occurred at 300~700 μm inside the biofilm, and denitrifying bacteria might be enriched in this range, this result was similar to the previous studies [30].

The variation of NO_3^--N and NO_2^--N was different at different C/N. Specifically, NO_3^--N decreased from 37.56 mg/L to 32.6 mg/L and NO_2^--N increased from 0 mg/L to 4.49 mg/L in the biofilm with C/N of 2. When the influent C/N increased to 6, NO_3^--N decreased from 37.53 mg/L to 26.73 mg/L and NO_2^--N increased from 0 mg/L to 9.25 mg/L. This was mainly because the limited carbon source at low C/N was consumed first with the decrease in DO, making carbon source insufficient for the denitrification. Moreover, efficient NO_2^--N production was obtained at all C/N ratio.

CO_2 is produced in the process of reducing NO_3^--N to NO_2^--N by organic carbon source, and the dissolved CO_2 in water will affect the acid-base balance by producing H^+. OH^- is produced during NO_2^--N reduction, resulting in a significant increase of pH value [7]. In the initial stage, the NO_3^--N reduction rate was much higher than the NO_2^--N reduction rate, so the pH decreased along the depth of the biofilm. When the influent C/N was 2, 3, and 6, the decrease in pH in the biofilm was significantly lower than that when the influent C/N was 4 and 5. This was because when the influent C/N was 2 or 3, the insufficient carbon source limited the NO_3^--N reduction, resulting in less CO_2 production. On the other side, when the influent C/N was 6, sufficient carbon source promoted the reduction of NO_2^--N and improved the OH^- production. Therefore, the decrease in pH in the biofilm was not significant when the influent C/N was low or high.

3.3. Effect of Influent pH on PD-MBBR

3.3.1. NO_2^--N Accumulation Performance

The effect of influent pH on the NO_2^--N production at PD-MBBR system was shown in Figure 6. Generally, stable NO_2^--N accumulation was achieved at all pH. When the influent pH value was 7, 8, and 9, the accumulation of NO_2^-N increased to the maximum at 30 min, reaching 29.26, 30.26, and 31.19 mg/L, respectively. It can be seen that with the increase in influent pH, the accumulation of NO_2^--N gradually increased, and the NO_2^--N concentration maintained at 24.20, 26.62, and 28.18 mg/L at the end of a cycle, respectively. But when the influent pH was 6, the reaction rate was relatively slow, resulting in the NO_2^--N peak occurring at 45 min with the NO_2^--N concentration of merely 27.14 mg/L. Moreover, at the end of the process, there was still 4.12 mg/L NO_3^--N remaining, indicating that the NO_3^--N reduction process was significantly inhibited under acidic conditions. Zhang et al. (2020) [12] also found similar results, that is, the denitrification process was significantly inhibited under acidic conditions, and the higher pH was more conducive to the accumulation of NO_2^--N under neutral and alkaline conditions with pH of 7.0~9.0. Previous study also proposed that the inhibition on copper type NO_2^--N reductase (NirK) activity under high pH condition was more significant [31]. Therefore, the highest NTR (96.49%) was obtained at a pH of 9.0. Further analysis found that the specific NO_2^--N reduction rate at the pH of 9 was the lowest (1.34 mg/(gVSS·h)), and over 83.2% of the influent NO_3^--N was converted to NO_2^--N at the end of the cycle. Therefore, a pH value of 9 was considered ideal for the NO_2^--N production in this study.

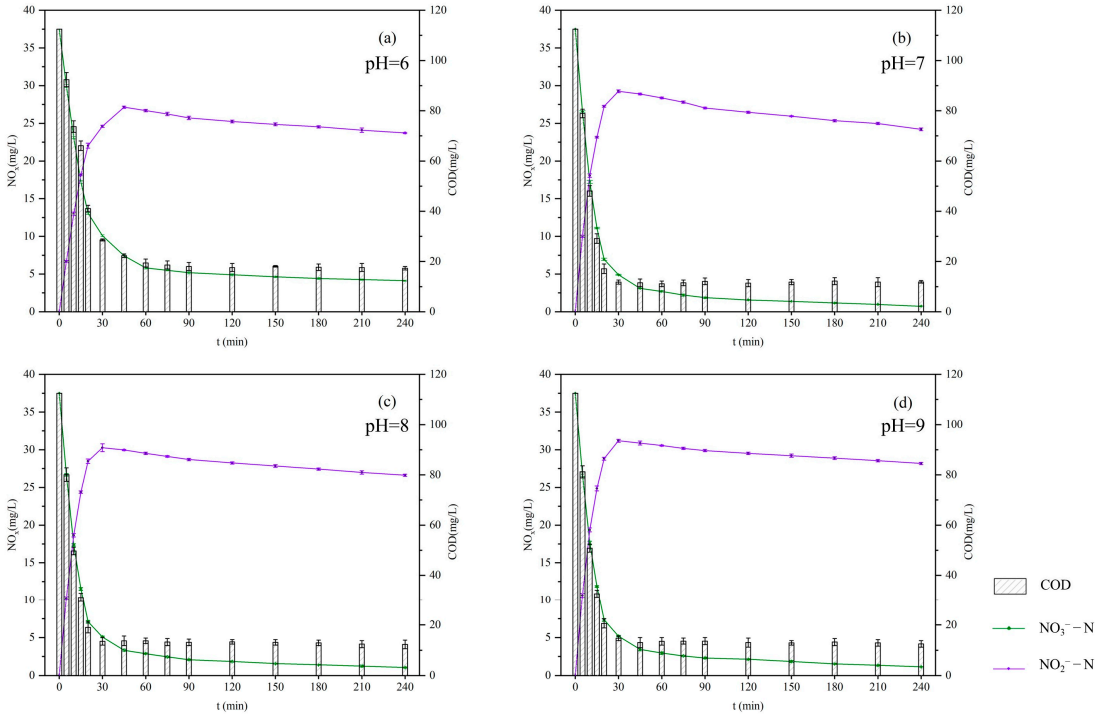

Figure 6. Changes of substrate concentration under different influent pH: (**a**) 6; (**b**) 7; (**c**) 8; (**d**) 9.

3.3.2. Microbial Community

The difference of microbial community structure in denitrifying MBBR under different influent pH was also studied. Generally, 46,660~54,206 valid sequences were obtained (Table 2). Chao index and Shannon index indicated that the total number of species and microbial diversity were the highest at the influent pH of 7, proving that the neutral environment was more conducive to the growth and reproduction of microorganisms.

Table 2. Alpha diversity of biofilm under different influent pH.

Sample	Reads	Index (Similarity: 97%)				
		OTU	Chao	Coverage	Shannon	Simpson
R1 (pH = 6)	54,206	442	480	0.999	4.17	0.0391
R2 (pH = 7)	51,309	464	484	0.999	4.38	0.0300
R3 (pH = 8)	46,660	440	479	0.999	4.16	0.0406
R4 (pH = 9)	49,194	431	454	0.999	4.10	0.0424

The relative abundance of biofilm microbial community structure at the genus level at different influent pH is shown in Figure 7. The relative abundance of *Saccharimonadales*, the dominant genus, was the lowest (32.73%) at the pH of 7. And when the influent pH increased to 9, its relative abundances increased to 39.89%. The abundance change of *Saccharimonadales* was closely correlated to the NTR in denitrification process, this uniformity proved the key roles of *Saccharimonadales* in partial denitrification. In addition, the relative abundance of *Comamonadaceae*, *Gemmobacter*, and other denitrifying bacteria in the acidic or alkaline environment was significantly lower, indicating that these bacteria were obviously suppressed at acidic or alkaline environment.

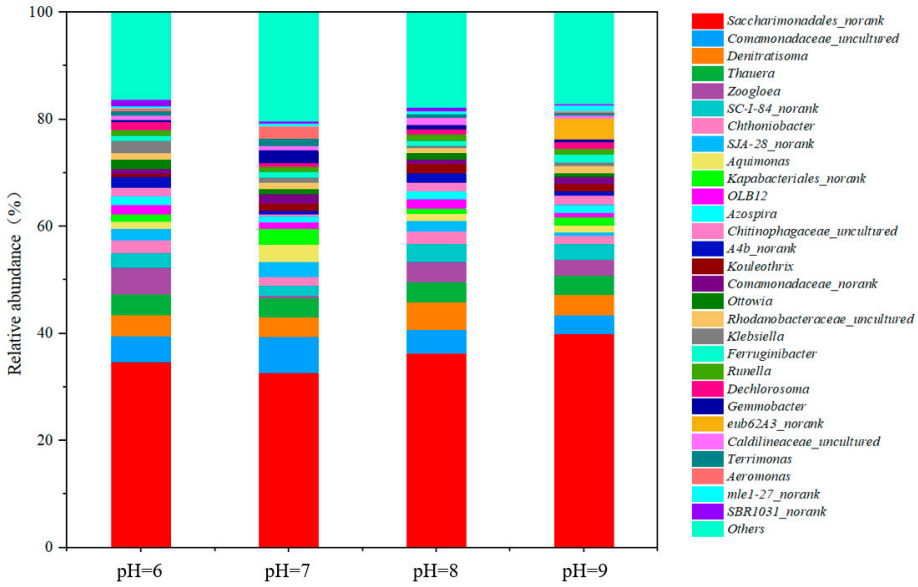

Figure 7. Microbial community structure of biofilm under different influent pH (genus level).

3.3.3. Biofilm Characteristic

The biofilm thickness on the carrier surface and the migration of substances inside the biofilm were analyzed (Figure 8). In the MBBR with influent pH 6, 7, 8, 9, the biofilm thickness was 1000, 1200, 1200, 1100 μm, respectively. The relative thicker biofilm at pH of 7 and 8 indicated the neutral or alkaline environment was more conducive to the growth of microorganisms. Inside the biofilm, NO_3^--N decreased greatly in the range of 300~700 μm inside the biofilm, and NO_2^--N accumulated continuously. Similar to the results in Section 3.3.1, the most efficient NO_2^--N production was observed when the influent pH was 9.

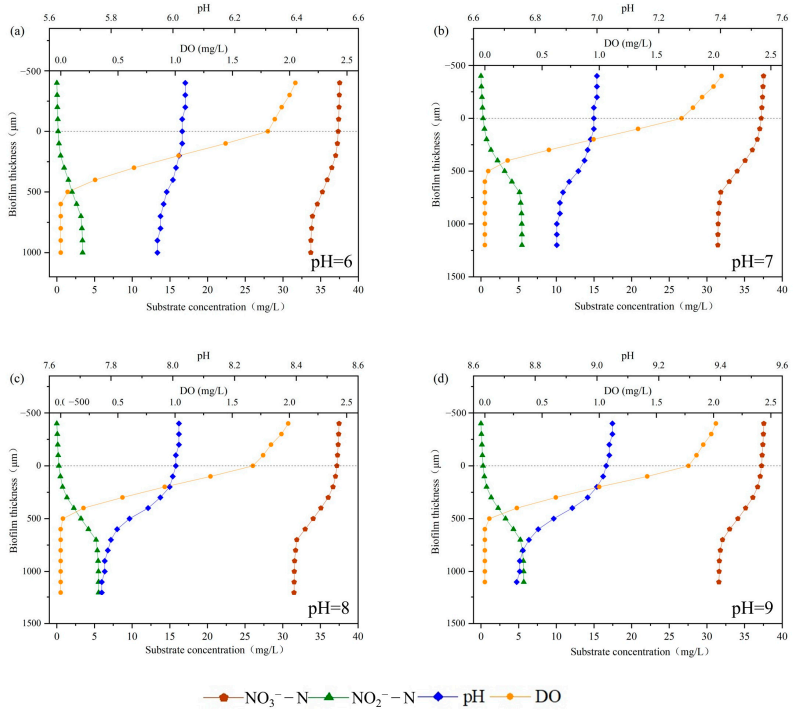

Figure 8. Biofilm thickness and the variation of substrate at different influent pH: (**a**) 6; (**b**) 7; (**c**) 8; (**d**) 9.

4. Conclusions

Efficient nitrite production with the NTR of 96.49% was achieved by C/N (3) and pH (9) control after the mature denitrifying biofilm was successfully formed in the biocarriers. *Saccharimonadales* was considered to be the key microbes with the relative abundance of 21.25–39.89%, which was closely related to the nitrite accumulation performance. Analysis about the biofilm characteristics found that the nitrite production efficiencies in the biofilm directly affected the performance of PD-MBBRs, and an anoxic environment in the biofilm (300~700 μm) was necessary for the PD reaction. This study confirmed the feasibility of PD-MBBR system for efficient nitrite production, providing a theoretical basis for the development of PD-Anammox technology in MBBR.

Author Contributions: Conceptualization, H.L.; Methodology, Z.X. and T.L.; Software, T.L. and Z.H.; Formal analysis, Z.H.; Investigation, Z.H.; Data curation, T.Y.; Writing—original draft, H.L.; Visualization, Z.X. and T.Y. All authors have read and agreed to the published version of the manuscript.

Funding: This research received no external funding.

Data Availability Statement: Supporting data can be found by emailing: zhangvladimir@163.com.

Conflicts of Interest: The authors declare no conflict of interest.

References

1. Mulder, A.; van de Graaf, A.A.; Robertson, L.A.; Kuenen, J.G. Anaerobic ammonium oxidation discovered in a denitrifying fluidized bed reactor. *FEMS Microbiol. Ecol.* **1995**, *16*, 177–183. [CrossRef]
2. Cao, Y.; van Loosdrecht, M.C.; Daigger, G.T. Mainstream partial nitritation-anammox in municipal wastewater treatment: Status, bottlenecks, and further studies. *Appl. Microbiol. Biotechnol.* **2017**, *101*, 1365–1383. [CrossRef]
3. Wang, J.; Li, L.; Liu, Y.; Li, W. A review of partial nitrification in biological nitrogen removal processes: From development to application. *Biodegradation* **2021**, *32*, 229–249. [CrossRef]
4. Granger, J.; Ward, B.B. Accumulation of nitrogen oxides in copper-limited cultures of denitrifying bacteria. *Limnol. Oceanogr.* **2003**, *48*, 313–318. [CrossRef]
5. Zhang, Z.; Zhang, Y.; Chen, Y. Recent advances in partial denitrification in biological nitrogen removal: From enrichment to application. *Bioresour. Technol.* **2020**, *298*, 122444. [CrossRef]
6. Ji, J.; Peng, Y.; Wang, B.; Mai, W.; Li, X.; Zhang, Q.; Wang, S. Effects of salinity build-up on the performance and microbial community of partial-denitrification granular sludge with high nitrite accumulation. *Chemosphere* **2018**, *209*, 53–60. [CrossRef]
7. Du, R.; Peng, Y.; Cao, S.; Li, B.; Wang, S.; Niu, M. Mechanisms and microbial structure of partial denitrification with high nitrite accumulation. *Appl. Microbiol. Biotechnol.* **2016**, *100*, 2011–2021. [CrossRef] [PubMed]
8. Cao, S.; Li, B.; Du, R.; Ren, N.; Peng, Y. Nitrite production in a partial denitrifying upflow sludge bed (USB) reactor equipped with gas automatic circulation (GAC). *Water Res.* **2016**, *90*, 309–316. [CrossRef] [PubMed]
9. Eskicioglu, C.; Galvagno, G.; Cimon, C. Approaches and processes for ammonia removal from side-streams of municipal effluent treatment plants. *Bioresour. Technol.* **2018**, *268*, 797–810. [CrossRef]
10. Du, R.; Cao, S.; Li, B.; Niu, M.; Wang, S.; Peng, Y. Performance and microbial community analysis of a novel DEAMOX based on partial-denitrification and anammox treating ammonia and nitrate wastewaters. *Water Res.* **2017**, *108*, 46–56. [CrossRef]
11. Qian, W.; Ma, B.; Li, X.; Zhang, Q.; Peng, Y. Long-term effect of pH on denitrification: High pH benefits achieving partial-denitrification. *Bioresour. Technol.* **2019**, *278*, 444–449. [CrossRef] [PubMed]
12. Zhang, T.; Cao, J.; Zhang, Y.; Fang, F.; Feng, Q.; Luo, J. Achieving efficient nitrite accumulation in glycerol-driven partial denitrification system: Insights of influencing factors, shift of microbial community and metabolic function. *Bioresour. Technol.* **2020**, *315*, 123844. [CrossRef]
13. Li, W.; Lin, X.Y.; Chen, J.J.; Cai, C.Y.; Abbas, G.; Hu, Z.Q.; Zhao, H.P.; Zheng, P. Enrichment of denitratating bacteria from a methylotrophic denitrifying culture. *Appl. Microbiol. Biotechnol.* **2016**, *100*, 10203–10213. [CrossRef] [PubMed]
14. Xiujie, W.; Weiqi, W.; Jing, Z.; Siyu, W.; Jun, L. Dominance of *Candidatus saccharibacteria* in SBRs achieving partial denitrification: Effects of sludge acclimating methods on microbial communities and nitrite accumulation. *RSC Adv.* **2019**, *9*, 11263–11271. [CrossRef] [PubMed]
15. Zhang, Q.H.; Yang, W.N.; Ngo, H.H.; Guo, W.S.; Jin, P.K.; Dzakpasu, M.; Yang, S.J.; Wang, Q.; Wang, X.C.; Ao, D. Current status of urban wastewater treatment plants in China. *Environ. Int.* **2016**, *92–93*, 11–22. [CrossRef]
16. Ødegaard, H. A road-map for energy-neutral wastewater treatment plants of the future based on compact technologies (including MBBR). *Front. Environ. Sci. Eng.* **2016**, *10*, 7–23. [CrossRef]
17. Pan, D.; Shao, S.; Zhong, J.; Wang, M.; Wu, X. Performance and mechanism of simultaneous nitrification–denitrification and denitrifying phosphorus removal in long-term moving bed biofilm reactor (MBBR). *Bioresour. Technol.* **2022**, *348*, 126726. [CrossRef]

18. Liu, Q.; Hou, J.; Zeng, Y.; Xia, J.; Miao, L.; Wu, J. Integrated photocatalysis and moving bed biofilm reactor (MBBR) for treating conventional and emerging organic pollutants from synthetic wastewater: Performances and microbial community responses. *Bioresour. Technol.* **2023**, *370*, 128530. [CrossRef]
19. Lawson, C.E.; Wu, S.; Bhattacharjee, A.S.; Hamilton, J.J.; McMahon, K.D.; Goel, R.; Noguera, D.R. Metabolic network analysis reveals microbial community interactions in anammox granules. *Nat. Commun.* **2017**, *8*, 15416. [CrossRef]
20. Kuenen, J.G. Anammox bacteria: From discovery to application. *Nat. Rev. Microbiol.* **2008**, *6*, 320–326. [CrossRef]
21. APHA. *Standard Methods for the Examination of Water and Wastewater*, 21st ed.; American Public Health Association: Washington, DC, USA, 2005.
22. Zhang, T.; Cao, J.; Liu, W.; Liu, G.; Huang, C.; Luo, J. Insights into integrated glycerol-driven partial denitrification-anaerobic ammonium oxidation system using bioinformatic analysis: The dominance of Bacillus spp. and the potential of nitrite producing via assimilatory nitrate reduction. *Sci. Total Environ.* **2023**, *858*, 160048. [CrossRef]
23. Mahto, K.U.; Das, S. Bacterial biofilm and extracellular polymeric substances in the moving bed biofilm reactor for wastewater treatment: A review. *Bioresour. Technol.* **2022**, *345*, 126476. [CrossRef] [PubMed]
24. Gong, L.; Huo, M.; Yang, Q.; Li, J.; Ma, B.; Zhu, R.; Wang, S.; Peng, Y. Performance of heterotrophic partial denitrification under feast-famine condition of electron donor: A case study using acetate as external carbon source. *Bioresour. Technol.* **2013**, *133*, 263–269. [CrossRef] [PubMed]
25. Albertsen, M.; Hugenholtz, P.; Skarshewski, A.; Nielsen, K.L.; Tyson, G.W.; Nielsen, P.H. Genome sequences of rare, uncultured bacteria obtained by differential coverage binning of multiple metagenomes. *Nat. Biotechnol.* **2013**, *31*, 533–538. [CrossRef] [PubMed]
26. Gu, Y.; Wei, Y.; Xiang, Q.; Zhao, K.; Yu, X.; Zhang, X.; Li, C.; Chen, Q.; Xiao, H.; Zhang, X. C:N ratio shaped both taxonomic and functional structure of microbial communities in livestock and poultry breeding wastewater treatment reactor. *Sci. Total Environ.* **2019**, *651*, 625–633. [CrossRef]
27. Remmas, N.; Melidis, P.; Zerva, I.; Kristoffersen, J.B.; Nikolaki, S.; Tsiamis, G.; Ntougias, S. Dominance of candidate Saccharibacteria in a membrane bioreactor treating medium age landfill leachate: Effects of organic load on microbial communities, hydrolytic potential and extracellular polymeric substances. *Bioresour. Technol.* **2017**, *238*, 48–56. [CrossRef]
28. Cao, J.; Zhang, T.; Wu, Y.; Sun, Y.; Zhang, Y.; Huang, B.; Fu, B.; Yang, E.; Zhang, Q.; Luo, J. Correlations of nitrogen removal and core functional genera in full-scale wastewater treatment plants: Influences of different treatment processes and influent characteristics. *Bioresour. Technol.* **2019**, *297*, 122455. [CrossRef]
29. Chen, J.; Strous, M. Denitrification and aerobic respiration, hybrid electron transport chains and co-evolution. *Biochim. Biophys. Acta* **2013**, *1827*, 136–144. [CrossRef]
30. Xue, Z.; Zhang, T.; Sun, Y.; Yin, T.; Cao, J.; Fang, F.; Feng, Q.; Luo, J. Integrated moving bed biofilm reactor with partial denitrification-anammox for promoted nitrogen removal: Layered biofilm structure formation and symbiotic functional microbes. *Sci. Total Environ.* **2022**, *839*, 156339. [CrossRef]
31. Du, R.; Peng, Y.; Ji, J.; Shi, L.; Gao, R.; Li, X. Partial denitrification providing nitrite: Opportunities of extending application for anammox. *Environ. Int.* **2019**, *131*, 105001. [CrossRef]